Use of seismic attributes to support fault tracing in Santos Basin Post-Salt sequences

Diório, G.R., UFPR; Trzaskos, B., UFPR; Assis, V. S. R., UFPR.

Abstract

Rheological properties of evaporites make salt diapirs important in tectonostratigraphic analyzes of sedimentary basins. Structurally, faults can nucleate in previous deformation events or be related to the rise of a salt diapir. Faults were mapped in a portion of the 3D seismic Block BS-500, Santos Basin, using the fault enhancement filter and the thinned fault likelihood attribute of the OpendTect software. Its use was important in separating conjugate faults in crestal grabens and regional normal faults near salt walls. The attributes helped recognizing main planes, geometries and fault continuity when integrated with stratigraphic features and the regional geological context.

Introduction

Evaporitic rocks that are predominantly made of halite (referred as *salt*) have distinct rheological properties, behaving like a fluid and deforming overlying rocks when under stresses (Hudec & Jackson, 2007). The structural aspects related to salt diapirs are important guides when analyzing the tectonostratigraphic evolution of a basin, especially because different situations trigger the beginning of salt tectonics. When the trigger is regional tectonics, salt responds to differential stress as a detachment surface, deforming preexisting structures or creating new ones (Jackson & Hudec, 2017). When buried, salt tends to become gravitationally unstable and move, deforming overlying rocks in a process called halokinesis (Hudec & Jackson, 2007), set off by slopes and/or different sedimentation rates overloading (Vendeville, 2005; Hude. & Jackson, 2007; Brun & Fort, 2011).

Separating such events becomes even more difficult in passive margin basins influenced by salt tectonics, as there are tectonic and non-tectonic triggers. In cases involving extensive tectonics and syndeformational sediment loading (see Hudec & Jackson, 2007; Caldas & Zalán, 2009; Brun & Fort, 2011), grabens’ formation sets off reactive diapirism (salt uses weakness zones to ascend), followed by an active stage (salt actively forces its way up to the surface), and may pass through a passive stage (emerging in the surface, advancing, and becoming allochthonous). For non-tectonic cases, different deformation domains are described, such as a proximal extension region, a transitional region and a distal shortening compressive region (Vendeville, 2005). Therefore, the recognition of the geometry of diapirs and faults helps to separate previous deformations from those generated by diapirism.

Santos Basin is a passive margin sedimentary basin known for being the one in the Brazilian coast with the largest volume of evaporites deposited in the Aptian and expressive salt tectonics (Pereira & Feijó, 1994; de Mio et al., 2005; Moreira et al., 2007), therefore relevant to study this subject. Its formation is related to the rupture of the Gondwana Supercontinent and the opening of the Atlantic Ocean, beginning in the Early Cretaceous (de Mio et al., 2005; Chang et al., 2008). The Neocomian rifting generated two main structural trends: NE-SW extensional faults, in Brasiliano weakness zones; and NW-SE transfer faults, which segmented the rift (Pereira et al. 1986; Meisling et al., 2001; Modica & Brush, 2004; Garcia et al., 2012). Salt tectonics generated an extensive and a compressive domain, separated by the Cabo Frio Fault, accounting for thin-skinned deformations in different types of basements (Guerra & Underhill, 2012, Garcia et al., 2012).

The use of 2D or 3D seismic surveys is extremely important in studies of salt tectonics since many of such basins rarely have outcrops. The objective of this work is to expose the methodology used during the tracing of faults existing in this context and to discuss the obtained results.

Methodology

The main material used was the BS-500 3D seismic block, which covers approximately 9,000 km². Within it, an area of ca. 1,120 km² was selected in the transition between the extensive and compressive salt domains in the southeast portion of the block, about 200 km from the capital of Rio de Janeiro (Fig. 1), with a range in time (depth) of 6,788 milliseconds (ms). In this area, seismic horizons and fault planes were interpreted in dGB Earth Science's OpendTect 6.6 Pro software. The methodology consisted of the detailed seismic interpretation of faults, with spacing between in-lines and cross-lines of 500 m.

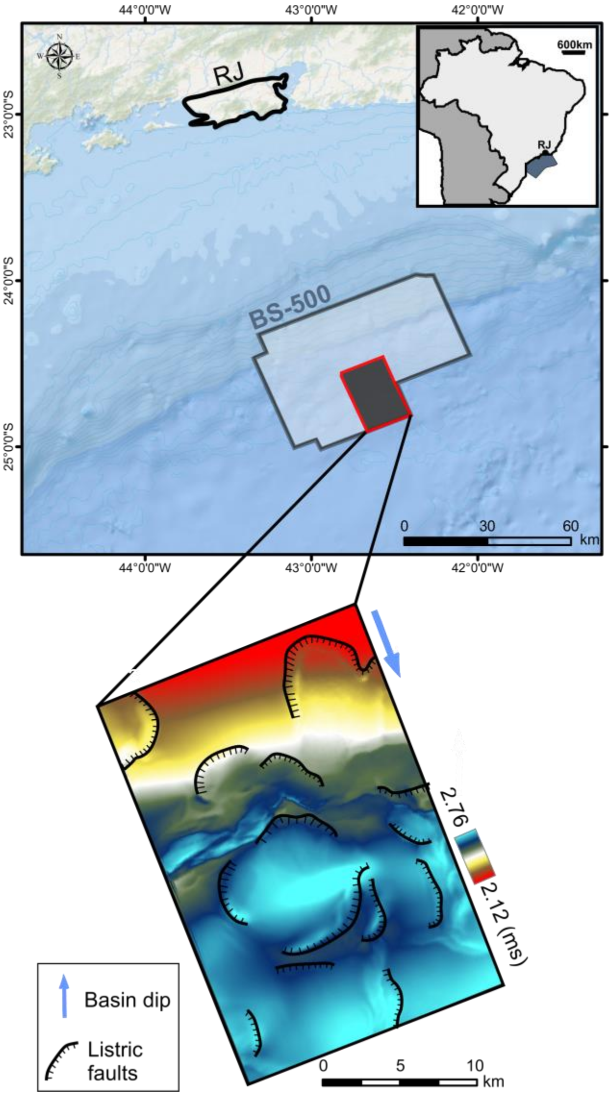

Figure 1 - Location of the studied area, including Santos Basin on the Brazilian coast (modified from Modica & Brush, 2004), the selected area (in red) in the BS-500 block and detail of the seabed relief with the traced listric faults.

Before tracing, plug-ins and attributes from OpendTect were created and later used (Fig. 2). The first was the dip steering plug-in, an algorithm that allows the creation of “steering cubes” that contain different local dip directions and azimuth of seismic events at each sample position, calculated considering spacings of 1 in in-line, cross-line and Z slice. The fault enhancement filter (FEF) was also used, which reduces random noise in areas close to faults and removes faultless discontinuities, based on diffusion filters (using the position attribute) and median dip (statistic attribute of the volume). Finally, the thinned fault likelihood (TFL) attribute is an algorithm that seeks to identify faults and fractures with the maximum similarity, using calculation steps of 2 for in-line and cross-line and values of 2, 16 (recommended by the manufacturer) and 32 for Z slice.

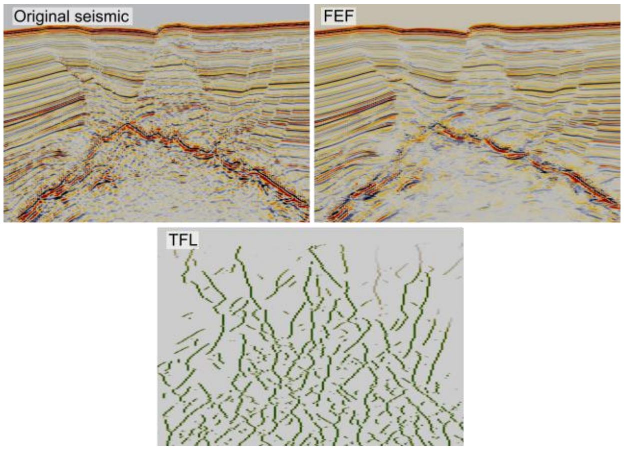

Figure 2 - Example of attributes used in in-line 1007. In this example the TFL was generated with the value 2 for Z slice

Results

A total of 160 fault planes were mapped, divided into three groups due to their geometries and sequences in which they occur: I) conjugated faults, anastomosed kilometric planes that form fault zones and crestal grabens in diapirs affecting all existing units in the area; II) regional normal faults of approximate N60E direction that affect all defined sequences; and III) low angle listric faults that deform only the most recent stratigraphic sequences.

The use of seismic attributes was especially important during the mapping and separation of Groups I and II. Both groups occur adjacent to salt walls (asymmetric linear bodies with no stock features in section) of preferential N30-60W direction, which are the largest diapiric features in the region with extensions between 6 and 10 km (see top of the salt in Fig. 3).

Considering the intrinsic relation between diapirism and fault formation, these groups were separated by correlating the after-processed seismic block with stratigraphic features. Stratigraphically, the main features analyzed were rollover anticlines, layer thickening and ramp-flat-ramp geometries (Fig. 3). Regarding the processed seismic attributes (Fig. 4), the TFL reinforced the existence of anastomosed faults above diapirs in Z slice and the use of the FEF helped highlighting the main faults existing in regions with multiple faults, especially near salt walls. It is worth noting that the TFL filter highlighted numerous penetrative anastomosed planes in Z slice, which made it impossible to trace each one individually, but the cross-line and in-line result was not used since the existence of multiple planes and discontinuities in the salt made it difficult to identify the main planes (see Fig. 2).

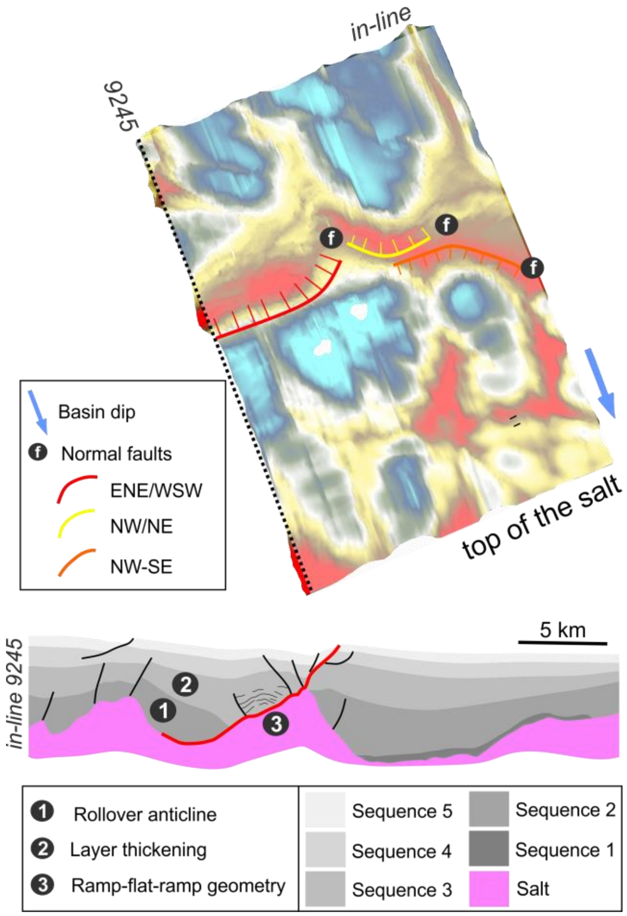

Figure 3 - Location of normal faults and examples of typical stratigraphic features on the ENE/WSW fault. In plan it is possible to perceive the relation between normal faults and salt walls existing in the region. Traced sedimentary sequences are highlighted in the in-line section.

Normal faults were mainly defined by typical stratigraphic features (see Fig. 3). Even though these faults have the greatest relative displacement of all, it is difficult to determine characteristics such as dip and continuity because salt diapirs and crestal grabens occur in these regions. Therefore, its seismic interpretation was restricted to the three largest and main faults.

As anastomosed conjugate fault zones are related to diapirs, the direction of the planes varied, but they are commonly synthetic and antithetic faults with displacements between the hanging wall block and the foot wall block reaching up to 400 ms.

The traced seismic horizons and sedimentary sequences (see in-line section in Fig. 3) were correlated with formal geological units, based on the classification proposed by Assine et al. (2008) and the seismic profiles of Caldas & Zalán (2009) and Guerra & Underhill (2012). H1 represents the contact between the Guarujá and Itanhaem Formations, while the others represent unconformities within the Itajaí-Açu (H2), Marambaia (H3 and H4) and Sepetiba (seabed) Formations. Therefore, Sequence 1 is within the Albian, Sequence 2 represents the Albian until the Campanian (Upper Cretaceous), Sequence 3 constitutes the Maastrichian to Rupelian (Upper Cretaceous and most of the Paleogene), Sequence 4 the Chattian until Serravallian (Oligocene to Middle Miocene) and Sequence 4 represents the Middle Miocene to the end of the Quaternary.

Discussion and Conclusions

The use of seismic attributes made it easier to trace existing faults nearby diapirs in the recognition of main planes (FEF) and in the perception of geometries and continuity of conjugated faults in Z slice (TFL). However, this tracing was only possible when integrating these data with stratigraphic features typical of fault zones and the regional geological context.

From a structural point of view, it was concluded that between the Albian and Upper Cretaceous normal antithetic faults were nucleated in the ENE/WSW direction (rollover anticlines), correlated to the Cabo Frio Fault, inciting a predominantly reactive diapirism phase. The passage from the Cretaceous to the Paleogene is marked by sedimentation concomitant with the development of normal ENE/WSW faults (layer thickening) and nucleation of normal antithetic NW/NE faults, which also incited reactive diapirism. Salt tectonics in the Cenozoic is marked by the collapse of diapirs and consolidation of crestal grabens, with formation of conjugated faults with anastomosing pattern and mock-turtle anticlines in N30-60W salt walls (see in-line 9245 in Fig. 3). Synthetic normal faults (NW/SE) were formed in the Oligocene. Formed from the Neogene, listric faults that deform recent non-lithified sediments indicate that salt tectonics remain active (see Fig. 1 and in-line 9245 in Fig. 3)

Acknowledgements

Authors are grateful to the *Agência Nacional do Petróleo, Gás Natural e Biocombustíveis* (ANP) for providing the used seismic data (Request 9359 - ANP Protocol nº 136867/2018) and dGB Earth Science for providing a remote use license for the OpendTect Pro. GRD is a master's student who thanks PETROBRAS for a scholarship. VSRA is a master's student who thanks *Coordenação de Aperfeiçoamento Pessoal de Nível Superior* - Brasil (CAPES) and PETROBRAS for scholarships. BT is a CNPq researcher (PQ 306780/2019-4).

References

Assine M. L., Corrêa F. S., Chang H. K. 2008. Migração de depocentros na Bacia de Santos: importância na exploração de hidrocarbonetos. Revista Brasileira de Geociências, 38(2 suppl): 111-127.

Brun J. P., Fort X. 2011. Salt tectonics at passive margins: Geology versus models. Marine and Petroleum

Geology, 28(6):1123-1145. doi.org/10.1016/j.marpetgeo.2011.03.004

Caldas M. F., Zalán P. V. 2009. Reconstituição cinemática e tectono-sedimentação associada a domos salinos nas águas profundas da Bacia de Santos, Brasil. Boletim de Geociências da Petrobras, 17(2): 227-248.

Chang H. K., Assine M. L., Corrêa F. S., Tinen J. S., Vidal A. C., Koike L. 2008. Sistemas petrolíferos e modelos de acumulação de hidrocarbonetos na Bacia de Santos. Revista Brasileira de Geociências, 38(2 suppl): 29-46.

de Mio E. D., Chang H. K., Corrêa F. S. 2005. Integração de métodos geofísicos na modelagem crustal da Bacia de Santos. Revista Brasileira de Geofísica, 23(3): 275-284. doi.org/10.1590/S0102-261X2005000300006

Garcia S. F. M., Letouzey J., Rudkiewicz J. L., Danderfer Filho A., Lamotte D. F. 2012. Structural modeling based on sequential restoration of gravitational salt deformation in the Santos Basin (Brazil). Marine and Petroleum Geology, 35(1): 337-353. doi.org/10.1016/j.marpetgeo.2012.02.009

Guerra M. C., Underhill J. R. 2012. Role of halokinesis in controlling structural styles and sediment dispersal in the Santos Basin, offshore Brazil. Geological Society, London, Special Publications, 363(1): 175-206. doi.org/10.1144/SP363.9

Hudec M. R., Jackson M. P. 2007. Terra infirma: Understanding salt tectonics. Earth-Science Reviews, 82(1-2): 1-28. Doi.org/10.1016/j.earscirev.2007.01.001

Jackson M. P., Hudec M. R. 2017. Salt tectonics: Principles and practice. Cambridge University Press. 516pp.

Meisling K. E., Cobbold P. R., Mount V. S. 2001. Segmentation of an obliquely rifted margin, Campos and Santos basins, southeastern Brazil. AAPG Bulletin, 85(11): 1903-1924. https://doi.org/10.1306/8626D0A9-173B-11D7-8645000102C1865D

Modica C. J., Brush E. R. 2004. Postrift sequence stratigraphy, paleogeography, and fill history of the deep-water Santos Basin, offshore southeast Brazil. AAPG Bulletin, 88(7): 923-945. https://doi.org/10.1306/01220403043

Moreira J. L. P., Madeira C. V., Gil J. A., Machado M. A. P. 2007. Bacia de Santos. Boletim de Geociencias da Petrobras, 15(2): 531-549.

Pereira M. J., Feijó F. J. 1994. Bacia de Santos. Boletim de Geociencias da Petrobras, 8(1): 219-234.

Pereira M. J., Barbosa C. M., Agra J., Gomes J. B., Aranha L. G. F., Saito M., Ramos M. A., de Carvalho M. D., Stamato M., Bagni, O. 1986. Estratigrafia da Bacia de Santos: análise das sequências, sistemas deposicionais e revisão litoestratigráfica. Congresso Brasileiro de Geologia, 34(1): 65-79.

Vendeville B. C. 2005. Salt tectonics driven by sediment progradation: Part I—Mechanics and kinematics. AAPG Bulletin, 89(8): 1071-1079. doi.org/10.1306/03310503063

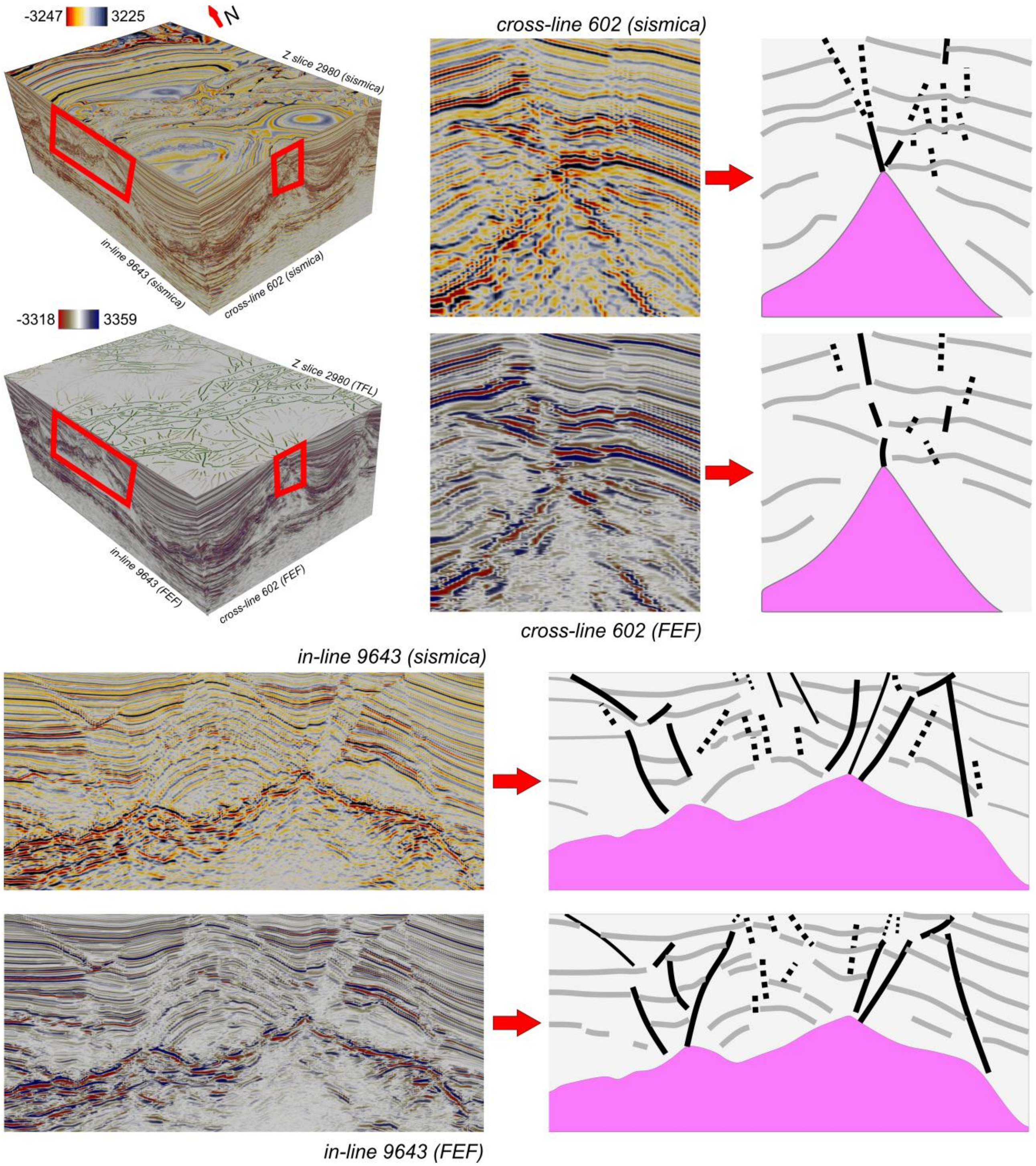

Figure 1 - Differences between the original seismic block and after its processing with the FEF (used mainly in in-lines and cross-lines) and the TFL (used in Z slice). Interpretations performed on in-lines of normal and conjugated faults were also added.